Atomistic study on the effect of the size of diamond abrasive particle during polishing of stainless steel

Prabhat Ranjan [1,2*], Anuj Sharma [3], Tribeni Roy [3,4]

[1]Bhabha Atomic Research Centre Mumbai, India, 400085
[2]Homi Bhabha National Institute Mumbai, India, 400094
[3]Department of Mechanical Engineering, BITS Pilani, India, 333031
[4]School of Engineering, London South Bank University, 103 Borough Road, London SE1 0AA, UK

* Corresponding author email address: pranjan@barc.gov.in

Abstract
Nanofinishing or polishing helps to reduce surface roughness which further improves both optical as well as chemical properties of engineering materials. During polishing of any engineering material, size of abrasive particles plays a significant role in efficient polishing. In this paper, stainless steel 304 (or SS304) is selected for polishing through diamond abrasive with varying particle size using molecular dynamics (MD) simulations. It is found that the diamond abrasive particle initially causes elastic deformation due to the attractive force between abrasive particle and the workpiece surface. As the size of the abrasive particle increases, plastic deformation occurs by spreading the dislocations on the surface only which helps to annihilate the dislocations after polishing. It is revealed that the smaller abrasive particles (less than 3 nm) get trapped due to strong chemically bonding with the surface of workpiece and the abrasive particles start depositing on the workpiece instead of material removal. In this paper, it is proposed that an optimum size of abrasive particles is required for a given set of polishing parameters towards efficient material removal and minimum surface/sub-surface defects. Thus, the present study is worthwhile for efficient polishing or nano-cutting of stainless steel through monocrystalline diamond.

Keywords: Nano-finishing, polishing, molecular dynamics simulation, stainless steel, LAMMPS, material removal

1. Introduction

Stainless steel is the most commonly used material for a wide range of industrial applications due to their amenable properties for various point of view such as high thermal conductivity, bio-compatibility, high melting point, high ductility etc. [1]. In stainless steel, there is a wide variants of alloy available and AISI 304L or SS304 with low carbon content is one of the most frequently used materials in industries due to its weldability, machinability, etc. [2]. In addition, this grade of steel is adaptable to improve surface finish after polishing to cater some specific applications where optically polished surface is required such as pressure gauges, optical sensors, surgical tools, biomedical implants, etc. [3–5]. To carry out the polishing operation, mechanical polishing through traditional lapping is often adopted in industries. The polishing process has also shown its another beneficial attribute to reduce the risk of corrosion by reducing surface roughness. Mechanical polishing at nanometric scale rearrange atoms on the surface in natural way by using thermal or chemical processes that enhances corrosion resistance drastically.

Polishing is also known as a final operation of manufacturing stages, which reduces surface roughness value as low as a few nanometres to maintain the surface finish in nanometric scale

and high precision on dimension as well as form accuracy of parts. When traditional processes for mechanical polishing are investigated, it is found that they lead some amount of defects of the parts. For example, traditional lapping and grinding process maintain the surface in nanometric scale but it also introduces various types of surface defects and sub-surface damages which limits the corrosion resistivity life of the parts beyond a certain value [6,7].

In view of these issues, the traditional ways of polishing were modified and advanced polishing processes have been developed like chemo-mechanical polishing (CMP) to finish steel with surface finish up to 0.7 nm or better on AISI304L using silica abrasive [8,9]. It was also found that chemo-mechanical magnetorheological finishing (CMMRF) process can be used to generate surface finish better than 0.2 nm on SS304L [9] with silica abrasive particles. This has happened due to the chemical interaction of abrasive particles with workpiece to implement chemically assisted material removal from the surface of SS304L material, thus the surface and sub-surface damages have been mitigated. Where CMMRF process combines the characteristics of chemical mechanical polishing (CMP) and magneto-rheological finishing (MRF) processes [10] to utilise beneficial attributes of both chemical and mechanical effects during the material removal using flexible magnetic tool of MRF technique. MRF based finishing utilises Magnetorheological fluid (MR) under influence of magnetic field to control the finishing forces to control the material removal at nanometric scale. There are different types of processes based on the magnetorheological fluid including magnetorheological finishing, magnetorheological abrasive flow finishing, rotational magnetorheological abrasive flow finishing and ball end magnetorheological finishing for the applications towards polishing of various complex freeform components [11]. Apart from these MRF and CMMRF processes, abrasive flow finishing process is also best suitable process to polish steel using suitable medium and abrasive particle as this process was demonstrated to polish microholes in surgical stainless steel [12].

As far as abrasive material is concerned, diamond comes in top list due to it hardness, thermal conductivity, sharpness, etc. In order to understand the effect of diamond abrasive for polishing, a three-body mechanism of polishing on silicon with diamond abrasive was investigated using a molecular dynamics simulation [13]. In this study, graphene lubrication enhances the heat dissipation and helps to reduce surface defects and subsurface damage

Mechanical polishing on stainless steel with diamond abrasive was investigated through molecular dynamics simulation, and it is observed that the finishing force and velocity damage the diamond abrasive by altering its phase from diamond cubic to graphite [14]. In the same view, it is also found that the diamond also exhibits its behaviour to chemically interact with stainless steel which helps to polish steel efficiently. As far as size of abrasive particles are concerned, it also affects both surface finish as well surface damages. Thus there is a need to analyse the effect of the size of diamond abrasive while polishing steel at nanometric scale. However, there is a dearth of literature available to apply diamond abrasives for polishing of steel at nanometric scale. Hence, this paper is focused to investigate and establish the mechanism of material removal on steel using various sizes of diamond abrasive particles. The effect of diamond abrasive size is carried out using molecular dynamics simulation and the same is discussed in the following sections of this paper.

2. Methodology

In this section, details of molecular dynamics simulation (MDS) are presented and discussed as MDS is known as the best tool to investigate nanometric investigation for any polishing process [15–17]. Parameters of the simulation is shown in *Table 1*.

Table 1: Parameters of molecular dynamics simulation.

S.N.	Parameters	Value
1	Workpiece material	SS304L (Fe:70% Ni:10% Cr:20%)
2	Fixed base of workpiece	17.5 nm x 7.0 nm x 0.7 nm
3	Thermostat region of workpiece	A block of 17.5 nm x 7.0 nm x 4.9 nm
4	Newtonian region of workpiece	A block of 17.5 nm x 7.0 nm x 0.7 nm with a conical asperity of height = 3.5 nm, and base diameter = φ7.0 nm
5	Type of initial surface	Conical (sharp). It is incorporated to represent a rough surface
6	Lattice structure of workpiece	Face centre cubic (FCC) with Lattice constant =0.35 nm
7	Number of atoms on workpiece	78,030
8	Abrasive particles	Mono-crystalline Diamond (C)
9	Size of abrasive particle	1nm to 6nm
10	Lattice structure of abrasive	Diamond cubic (DC) with lattice constant =0.357nm
11	Finishing medium	Water. It regulates temperature of workpiece and abrasive at 300K
12	Time step	1 fs
13	Simulation time	47 ps
14	Viscous damping on abrasive	1.8×10^{-8} gm/s
15	Boundary	X: periodic, Y: periodic, Z: shrink

The MDS model consists of workpiece with a conical asperity, and abrasive particle as shown in *Fig.1*. To imitate water medium of polishing, entire system of simulation is put under consideration of cooling and damping. For example, temperature of thermostat and abrasive atoms were set to maintain 300K as water acts as an efficient coolant, and damping attribute of water was imposed on abrasive instead of direct modelling of water. The conical asperity is modelled to study the abrasion process on a rough surface. The conical asperity has sharp geometry at apex which would help to correlate this MDS phenomena on highly rough surface to investigate material removal and surface modification.

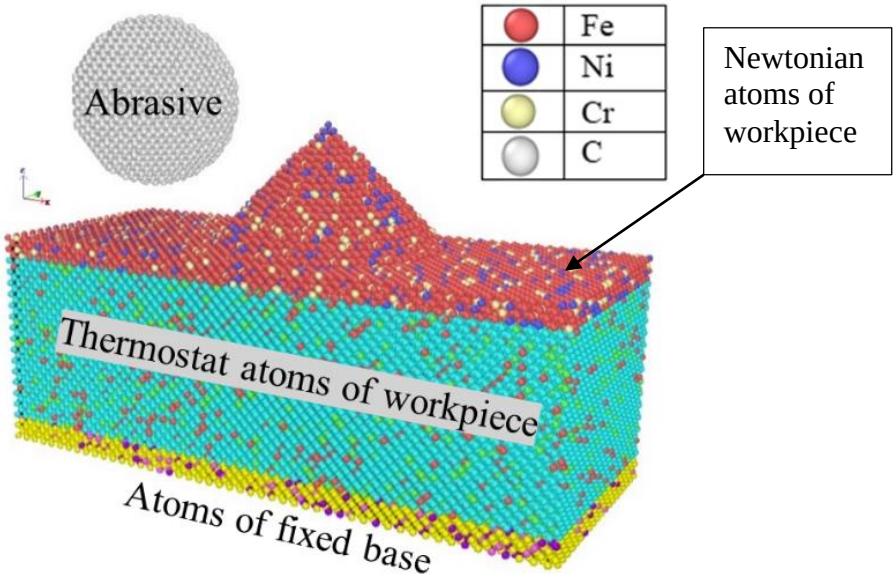

Fig. 1. MDS model for nanofinishing. Atom symbols are shown for Newtonian atoms and abrasive atoms

Motion and position of the Newtonian atoms of *Fig.1* are governed by Newton's second law of motion and fixed base atoms are frozen i.e. zero velocity. It was calculated by the direct

integration of the classical Hamiltonian equations of motion using the Velocity-Verlet algorithm. Nanofinishing process was simulated using constant micro-canonical ensemble (NVE) under a constant number of atoms (N), the system's volume (V) and the total energy in the system (E).

Table 2: Details of the pair potential to model and simulate materials in MDS.

S.N.	Atom-pair	Type of pair potential
1	Fe-Ni-Cr	EAM [18]
2	C-C	Tersoff [19]
3	C-Fe and C-Cr	Morse [20]
4	C-Ni	Morse [21]

To create inter-atomic forces, a hybrid pair potential was applied. This hybrid pair potential includes five types of pair potentials as shown in *Table 2*. Embedded atom method (EAM) type of pair potential was used to simulate stainless steel. For diamond abrasive particles, Tersoff potential was selected. Morse potential was used for the atoms of abrasive and workpiece. In the present work, LAMMPS software [22] was used to perform a series of simulations as per the *Table 1*. To implement LAMMPS for polishing, a model is constructed as per *Table1* and *Fig.1*, and it was equilibrated up to 2 picoseconds to stabilise potential energy of all atoms. Thereafter, dynamics of polishing was applied by incorporating indentation and linear translation of abrasive against the workpiece. To visualize the result of the simulation, OVITO software [23] was used, and further analysis was performed using post processing on the output data of the simulation. Towards better accuracy of the result with satisfactory computational efficiency, the computational time step was set to 1 fs. The abrasive particle was allowed to move under influence of an external force and viscous damping along *x*-axis. Size of the abrasive particle was varied from ϕ1 nm to ϕ6 nm with step of 1 nm, and the size of asperity of workpiece was set to 3.5 nm as in nanofinishing, material removal is of the order of a few nanometre or less.

3. MDS and analysis techniques

3.1 Temperature

In general, material removal zone in mechanical abrasion polishing is relatively low and it is experimentally difficult to measure the temperature. Hence, molecular dynamics simulation is used to calculate kinetic energy of the work-piece atoms for mapping the temperature at every time-step.

3.2 Atomistic stress

Interaction between atoms of abrasive and workpiece leads to stresses for deforming material. In general, virial stress [24] is used to compute stress on individual atoms. From the analysis point of view, von-Mises stress has been computed which tells about equivalent stress on a specific atom instead of having a set of stress matrix.

3.3 Common neighbor analysis

Structure analysis is an essential aspect to characterize arrangement of atoms for discriminating between several structures like FCC, BCC, HCP, DC, etc. through adaptive common neighbor analysis method [23].

3.4 Dislocation analysis

In this analysis all dislocation line and point defects in an atomistic crystal are computed with their Burgers vectors, and length of the dislocations. For computation, an automated algorithm

has been based on a discrete Burgers circuit integral over the elastic displacement field without limiting any specific lattices or dislocation types [25].

4. Results & discussion

After carrying out all simulations, suitable processing method was also implemented to analyse and investigate the process or behaviour of components. Afterwards, all results are discussed in the following sections.

4.1 Temperature

During entire period of polishing, temperature was computed on abrasive particle and workpiece, and maximum temperature is plotted, as presented in *Fig. 1*. It shows two different slopes. From 1 nm to 4 nm abrasive diameter, it displays small slope and the slope is increased after 4 nm, which indicates that the rise in temperature for abrasives with diameter less than 4nm leads to the pure chemical bonding between abrasive and workpiece. In case of bigger abrasive particle, mechanical deformation might be dominating over the temperature rise due to chemical bonding. For example, the maximum temperature is localised on the interface of abrasive and workpiece, and with 5nm particle, it shows the temperature spread beneath the interface as shown in the inset photos of *Fig.1*. This result indicates that the abrasive size up to 4 nm leads to the chemical interactions in majority which is surface to surface phenomenon. Hence, the material removal up to 4 nm particle size can be treated as free from mechanical deformation/damages to the workpiece.

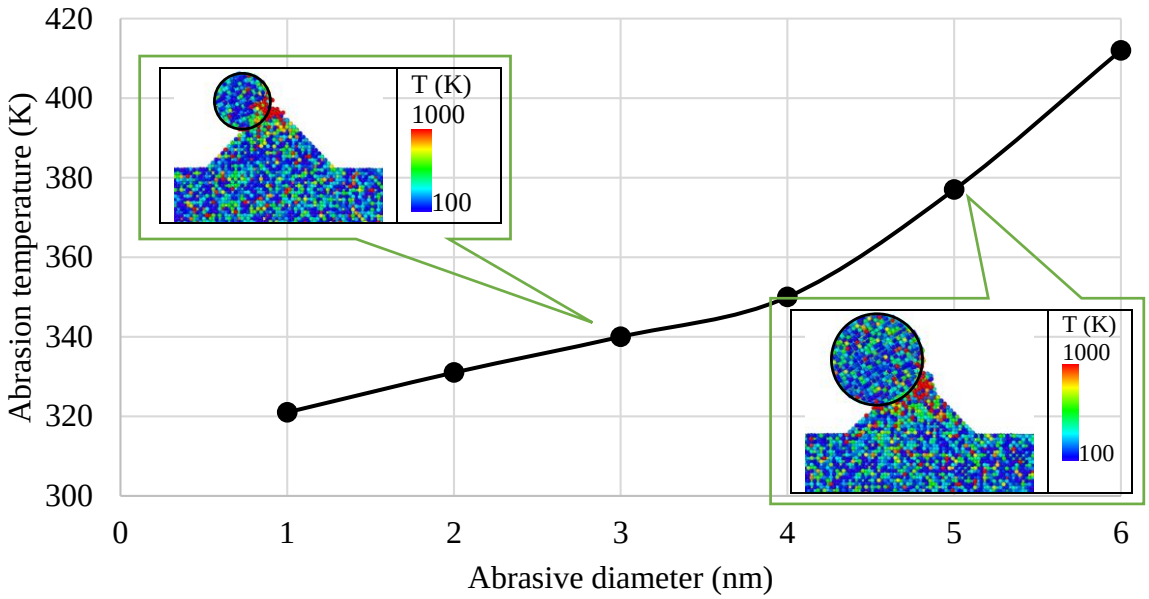

Fig.2: Abrasion temperature during polishing with varying diameter of diamond abrasives.

4.2 Mises stress

von-Mises stress is computed with different sizes of abrasive during polishing and after polishing to find residual stress as presented in *Fig. 3*. In this figure, atomistic Mises stress is also presented for both small as well as bigger abrasive particle in inset. The atomistic becomes about 70 GPa for both cases and it is enough to transform the lattice structure of abrasive and

workpiece as the material's lattice gets changed at the stress level more than their theoretical tensile strength ($E/2\pi$) [26].

The stress during polishing and the residual stress were computed by averaging out the atomistic von-Mises stress on the interaction zones of peak. *Fig.3* shows that the residual stress and stress during polishing become almost unchanged when the abrasive size is varied from 1 nm to 4 nm.

For the small size of abrasive, the atomistic Mises-stress is shown in an inset of *Fig.3* at diameter of 3 nm. This atomistic stress plot indicates that the stress is getting generated at the interface between abrasive and workpiece and it is also getting localised there itself. It means, small abrasive induces stress on the surface of workpiece only and the residual value is also on minimal side.

When size of abrasive increases further and reaches to bigger size, residual and Mises-stress of polishing also increase linearly, which starts after 4 nm size of diamond abrasive. To understand insight of the phenomenon, atomistic stress is presented in inset at diameter of 5 nm in *Fig.3*. The atomic stress shows that the stress spreads along the interface of abrasive and workpiece, and it also moves beneath of the work surface.

It can be stated that the size of abrasive helps to increase the contact surface which further leads to rise in the stress. Moreover, bigger abrasive particle applies more force, and due to this, stress travels further. The travel length beneath the work surface induces plastic deformation with phase transformation and sub-surface damages.

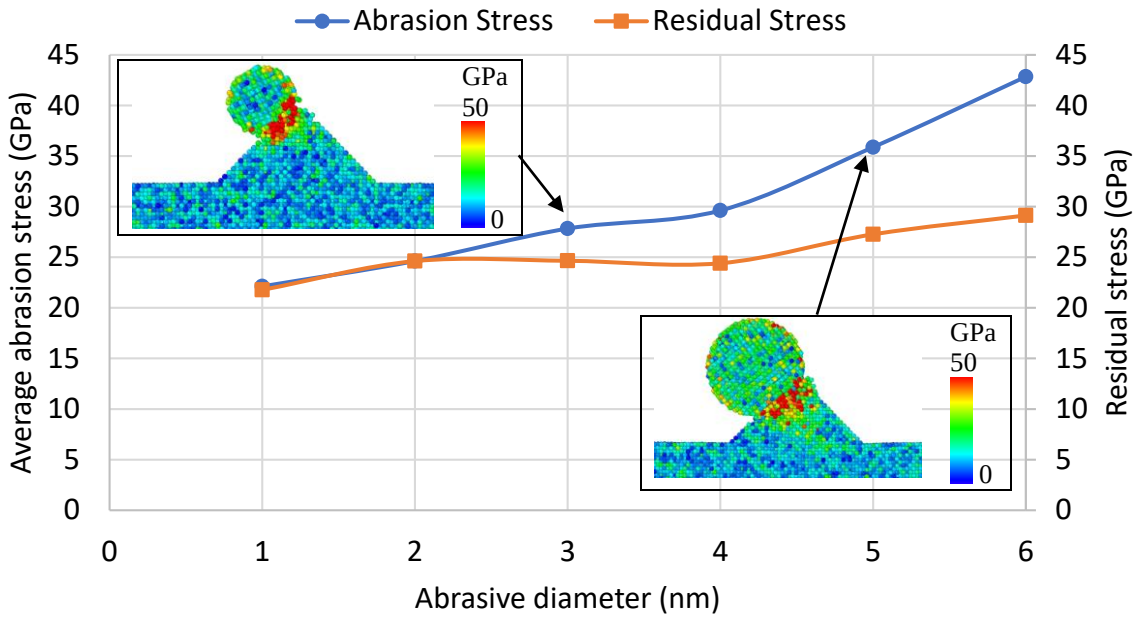

Fig.3: von-Mises stress during polishing and residual stress with varying diameter of diamond abrasives.

Based on the results obtained so far, it is essential to investigate the phenomena of plastic deformation further. Hence, phase transformation, lattice structure and dislocation analysis were carried out and presented as follows.

4.3 Phase transformation

It was found that smaller particle does apply plastic deformation and due to this smaller abrasive with abrasive size of 3nm and bigger abrasive with diameter 6 nm were selected to investigate the phase transformation on workpiece. Based on common neighbor analysis, lattice of workpiece and abrasive were computed and presented in *Figs. 4 and 5*.

Figs. 4(a-d) show lattice structure of workpiece and abrasive at 0 ps, 12 ps, 17 ps and 30 ps where the initial contact at 12 ps leads to a major amount of lattice transformation on the workpiece in HCP, BCC and amorphous structures. As time progresses, abrasive atoms also get affected as the circular shape of cubic diamond phase changes from *Fig. 4(a)* to *Fig. 4(b)*. *Fig. 3(d)* shows that the processed workpiece gets smoothened on the sharp conical asperity without any altered lattices. It is observed that during polishing, workpiece lattice phase is getting transformed from FCC to HCP, BCC and amorphous, and they are restricted on the work surface. This is happening due to pure rolling of abrasive as the contact region gets bonded as shown in *Fig. 4(d)*.

As small abrasive possesses more surface area, and results in high friction force from workpiece which helps to allow rolling movement of abrasive instead of sliding under specified inertia force. This phenomenon helps to carry out polishing of workpiece with rolling action of abrasive, and due to this, material removal takes place without any surface and sub-surface damages. Thus, smaller diamond abrasive is responsible to polish stainless steel surface with nano-metrically smooth surface without any sub-surface damages. However, the abrasive gets affected by its phase transformation and materials loading that needs attention to improve the polishing process.

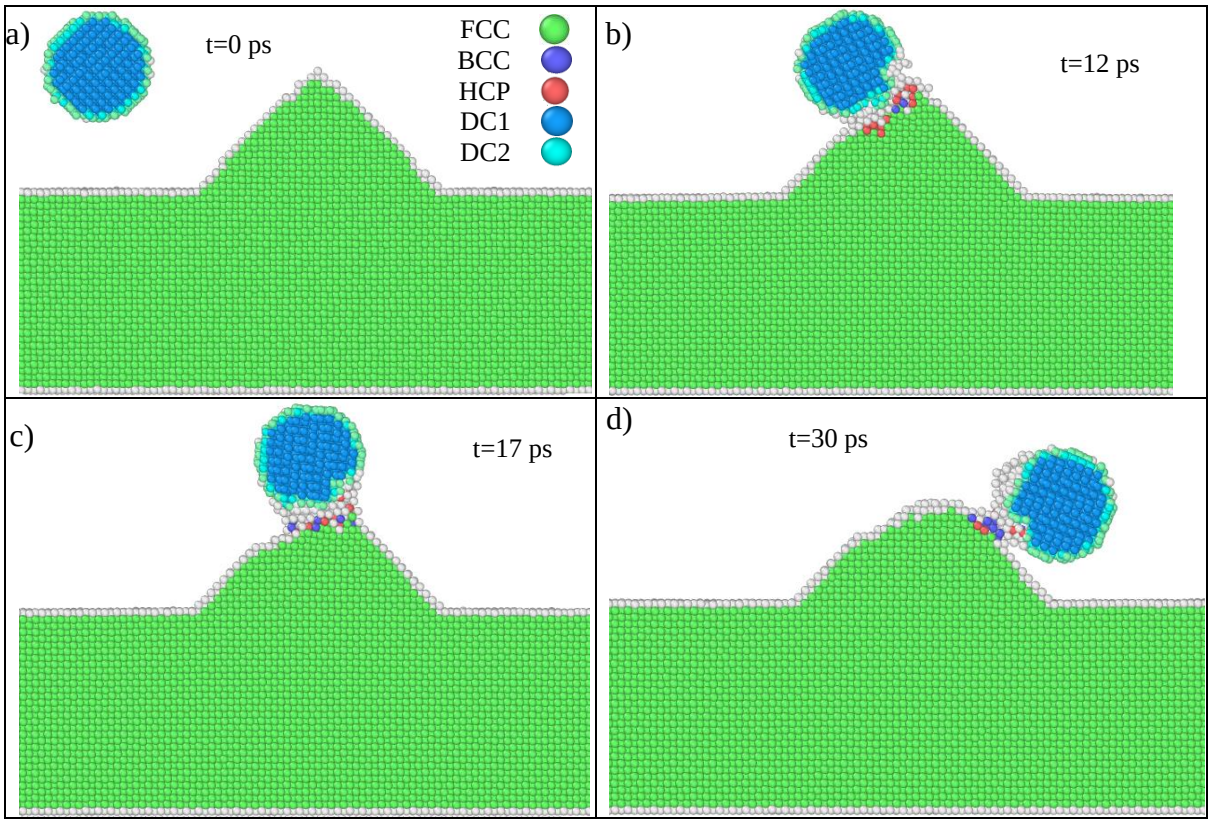

Fig.4: Lattice structure during polishing with small abrasive or the abrasives diameter of 3nm.

In case of bigger abrasive as shown in *Figs. 5(a-d)*, all phase transformation and material removal dynamics are similar except following attributes.

-Physical stability of abrasive: The lattice structure of abrasive with bigger size helps to reduce the surface area to volume ratio which further reduces the surface energy to get physically stable abrasive particle. This effect helps to deform the abrasive without damaging the lattice or phase of the abrasive, which can be called as elastic deformation.
- Sub-surface damages on the workpiece: Friction force majorly depends on the contact area and the contact area becomes low in case of bigger abrasive as bigger abrasive becomes more stable as discussed previously. Thus low friction force and high inertia force leads to the development of the phase transformation beneath the work surface while crossing the asperity of workpiece as shown in *Fig. 5(c)*.

While removal of material from workpiece, all transformed phases are taken away by abrasive as shown in the inset of *Fig. 5(d)*. But the deformed lattice on the abrasive remains in it with atoms adhered from workpiece.

To understand how the abrasive size can lead to the surface and sub-surface damages, it is better to analyse dislocation which is being induced within the workpiece during polishing.

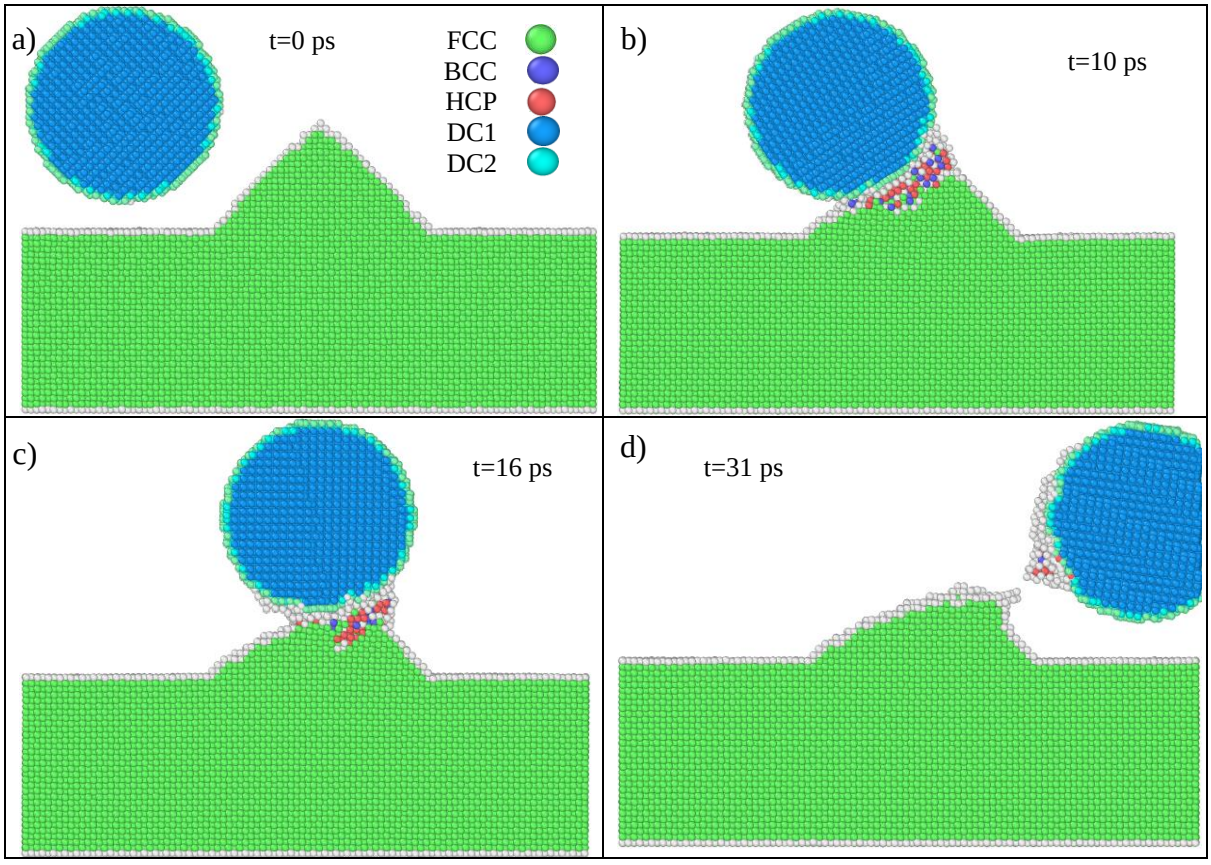

Fig.5: Lattice structure during polishing with bigger abrasive or the abrasives diameter of 6nm.

4.4 Dislocations

Fig. 6 shows the maximum length of dislocations which is being induced during entire course of polishing with respect to the size of abrasive particle.

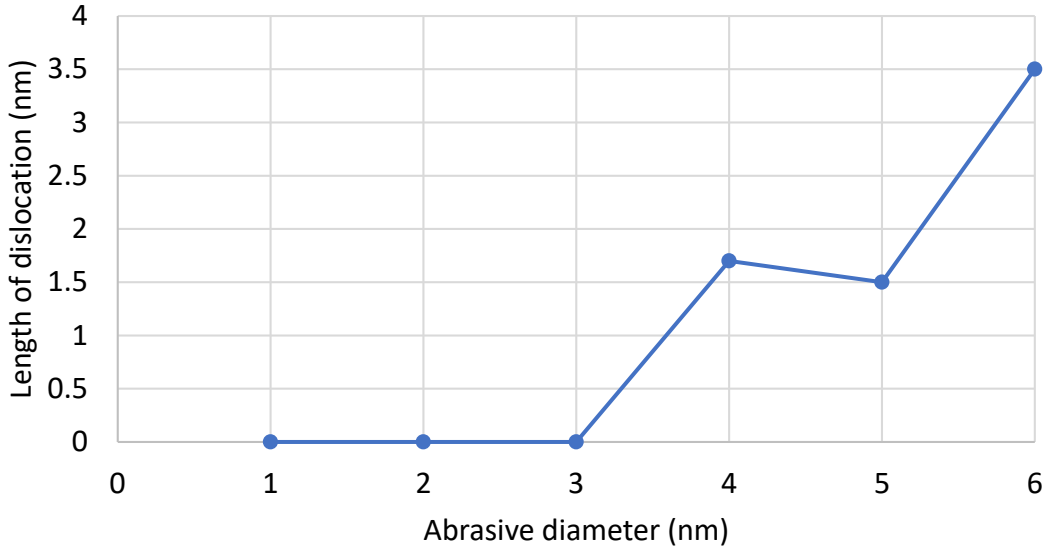

Fig.6: Length of dislocation induced during polishing with varying diameter of abrasive.

It is noticed that the dislocations start forming at the abrasive size equal to 4 nm and higher which leads to the plastic deformation when abrasive size more than 4nm, otherwise, it will be purely elastic deformation. As size of abrasive increases, dislocations start progressing rapidly which results in enormous plastic deformation. Thus, bigger abrasive can lead to the surface and sub-surface defects.

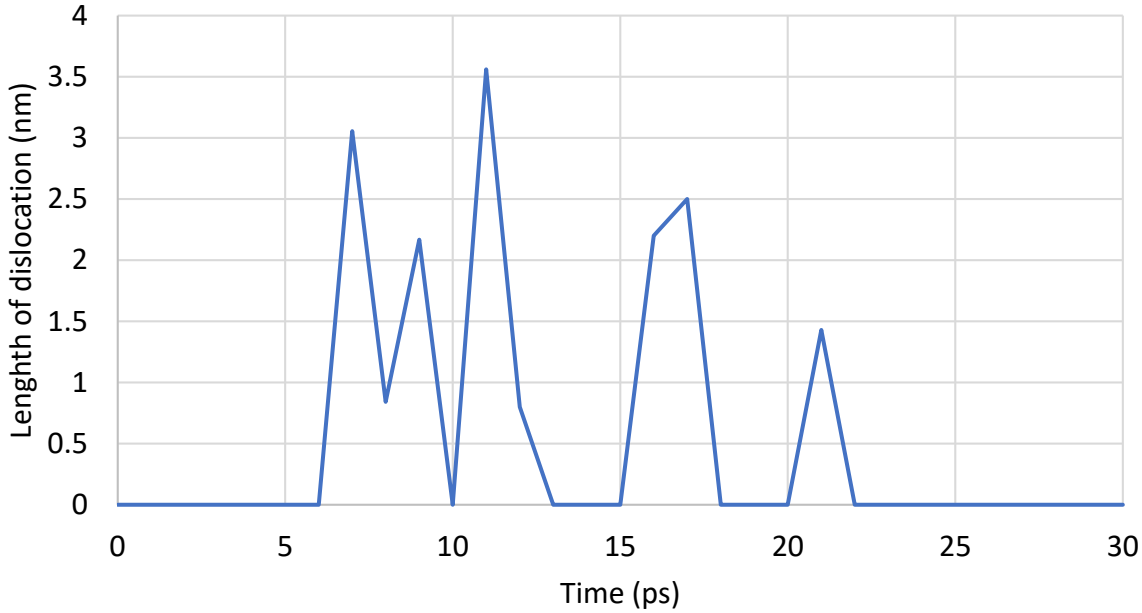

Fig.7: Length of dislocation induced during polishing at abrasive diameter of 6 nm.

To understand the sub-surface defects, it is important to analyse dislocations beneath the work surface. Hence, the dislocations at different time of polishing is computed and presented for the abrasive of 6 nm as presented in *Figs. 7 & 8*.

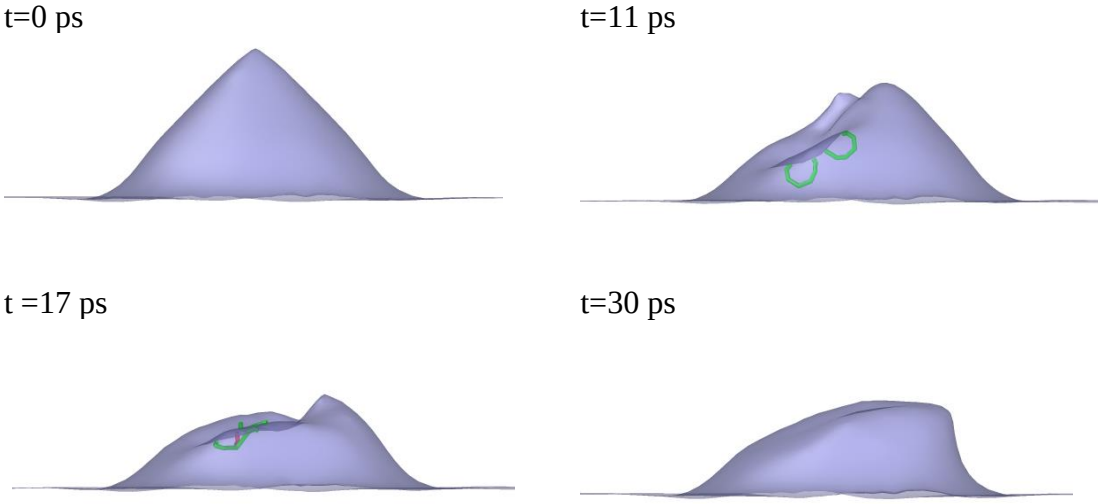

Fig.8: Dislocation induced during different time of polishing at abrasive diameter of 6 nm.

It is noticed that the 6 nm size abrasive leads to the formation of shockley dislocations (or movable dislocation) only which helps to move it up to the surface and annihilate itself as shown in *Figs. 8(a-d)*. This effect of induction and disappearance of dislocations happens in the present case of nano-sized diamond abrasive particles which induces movable dislocations near the work-surface for material deformation followed by material removal from the surface.

4.5 Material removal

As far as material removal is concerned, the displaced atoms from the work surface is plotted with respect to the abrasive diameter as presented in *Fig. 9*. This result shows that the material removal increases with abrasive diameter. But is not so as smaller abrasive particle does displacement of atoms but it does not remove atoms from work surface. At smaller abrasive, atoms of workpiece gets displaced from its region but they are not removed completely as shown in the inset snapshot at 2 nm of *Fig. 9*. In this case, 2 nm size abrasive is getting permanently fused with the asperity of workpiece which even not able to get removed from its own inertia force. When the abrasive size increases further, 3 nm abrasive is able to get detached from the work surface due to attaining enough inertia force on the abrasive as shown in the figure. Moreover, the smaller abrasive also gets damaged (in form of phase transformation of abrasive as shown in *Fig. 4 (b)*) when more force is applied to remove it.

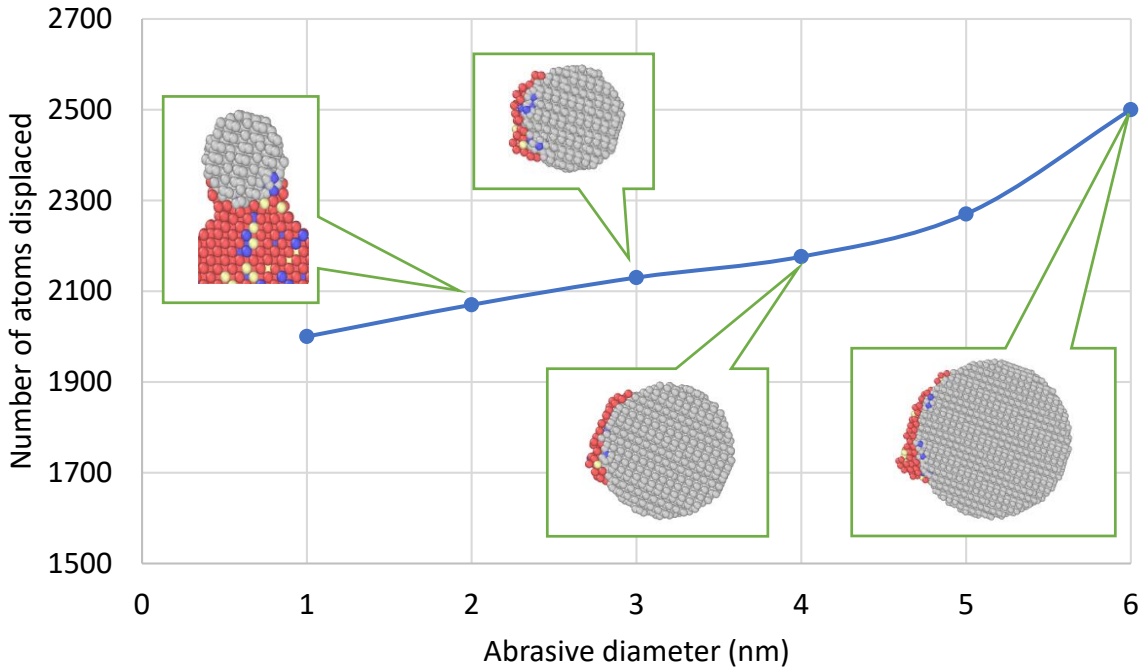

Fig.9: Lattice structure during polishing with bigger abrasive or the abrasives diameter of 3 nm.

Consequently, it can be stated that the material removal effectively starts from the abrasive particle size of 3 nm and higher. The abrasive with the diameter less than 3 nm leads to fusion or deposition with surface instead of abrasion action. Thus, the present work brings out following important attributes from the point of view of material removal.

1) Bigger abrasive leads to the surface and sub-surface defects.

2) Smaller abrasive gets fused on the work surface.

3) The abrasive size with 3 nm results material removal without formation of any dislocation. Hence, it can be called as elastic emission.

As far as experimental validation is concerned, it is almost impossible to investigate the interaction phenomenon of material removal, phase transformation, temperature, etc.at time scale of few picoseconds. However, the final effect of chemical bonding of diamond with steel matches with the literature [27].

Conclusions

In this paper, simulations at molecular scale were carried out to investigate the effect of the size of diamond abrasive particle for polishing of stainless steel. The conclusions are summarised as follows.

- During polishing, temperature increases linearly with abrasive size up to 4nm. Afterwards, the temperature increases with higher rate. The reason is that the material removal up to 4 nm can be treated as free from mechanical deformation/damages to the workpiece.

- The abrasive size from 1 to 4 nm induces stress on surface only which helps to minimise residual stress on workpiece. On other hand, bigger abrasive particle applies more force, and due to this, stress travels beneath the work surface which induces plastic deformation with phase transformation and sub-surface damages.

- The diamond abrasive becomes physically stabile in case of bigger size (more than 3 nm). In the same view, smaller abrasive is physically unstable and it helps to increase contact surface which tries to fuse the abrasive and removal of abrasive becomes extremely difficult.

- The abrasive with the diameter less than 3 nm leads to fusion or deposition with surface instead of abrasion action.

- Diamond abrasive size of 3 nm does material removal without formation of any dislocation. Hence, this size of abrasive is possible to realise elastic emission polishing of stainless steel.

- The abrasive size higher than 5 nm leads to low friction force and high inertia force which induces the phase transformation and dislocation formation beneath the work surface.

- Diamond abrasive with 6 nm size induces the formation of shockley dislocations during polishing and it gets annihilated on work surface after completion of polishing.

- Thus, the present work suggests that bigger abrasives are recommended for higher material removal. To reduce the surface and surface-defects, the polishing can be implemented with final stage of polishing using the abrasive diameter of 3 to 4 nm.

References

[1] E. V Zaretsky, Rolling bearing steels - a technical and historical perspective, Mater. Sci. Technol. 28 (2012) 58–69. doi:10.1179/1743284711Y.0000000043.

[2] S. Fatima, M. Khan, S.H.I. Jaffery, L. Ali, M. Mujahid, S.I. Butt, Optimization of process parameters for plasma arc welding of austenitic stainless steel (304 L) with low carbon steel (A-36), Proc. Inst. Mech. Eng. Part L J. Mater. Des. Appl. 0 (2015) 1464420715584392. doi:10.1177/1464420715584392.

[3] C.-C. Shih, C.-M. Shih, Y.-Y. Su, L.H.J. Su, M.-S. Chang, S.-J. Lin, Effect of surface oxide properties on corrosion resistance of 316L stainless steel for biomedical applications, Corros. Sci. 46 (2004) 427–441. doi:10.1016/S0010-938X(03)00148-3.

[4] V. Sansone, D. Pagani, M. Melato, The effects on bone cells of metal ions released from orthopaedic implants. A review, Clin. Cases Miner. Bone Metab. 10 (2013) 34–40. doi:10.11138/ccmbm/2013.10.1.034.

[5] S. Ghildiyal, P. Ranjan, S. Mishra, R. Balasubramaniam, J. John, Fabry-Perot Interferometer-Based Absolute Pressure Sensor With Stainless Steel Diaphragm, IEEE Sens. J. (2019). doi:10.1109/JSEN.2019.2909097.

[6] S. Gao, H. Li, H. Huang, R. Kang, Grinding and lapping induced surface integrity of silicon wafers and its effect on chemical mechanical polishing, Appl. Surf. Sci. (2022). doi:10.1016/j.apsusc.2022.153982.

[7] A. Esmaeilzare, A. Rahimi, S.M. Rezaei, Investigation of subsurface damages and surface roughness in grinding process of Zerodur ® glass-ceramic, Appl. Surf. Sci. (2014). doi:10.1016/j.apsusc.2014.05.137.

[8] X. Hu, Z. Song, W. Liu, F. Qin, Z. Zhang, H. Wang, Chemical mechanical polishing of stainless steel foil as flexible substrate, Appl. Surf. Sci. 258 (2012) 5798–5802. doi:10.1016/j.apsusc.2012.02.100.
[9] P. Ranjan, R. Balasubramaniam, V.K. Jain, Investigations into the mechanism of material removal and surface modification at atomic scale on stainless steel using molecular dynamics simulation, Philos. Mag. (2018). doi:10.1080/14786435.2018.1439191.
[10] Y. Kumar, H. Singh, Chemomechanical magnetorheological finishing: Process mechanism, research trends, challenges and opportunities in surface finishing, J. Micromanufacturing. 5 (2021) 193–206. doi:10.1177/25165984211038878.
[11] M. Kumar, H.N. Singh Yadav, A. Kumar, M. Das, An overview of magnetorheological polishing fluid applied in nano-finishing of components, J. Micromanufacturing. 5 (2021) 82–100. doi:10.1177/25165984211008173.
[12] S. Singh, M. Ravi Sankar, Development of polymer abrasive medium for nanofinishing of microholes on surgical stainless steel using abrasive flow finishing process, Proc. Inst. Mech. Eng. Part B J. Eng. Manuf. 234 (2019) 355–370. doi:10.1177/0954405419883768.
[13] H. Dai, W. Wu, Y. Hu, Lubricating effect of graphene during ultra-precision mechanical polishing by atomic scale simulation, Proc. Inst. Mech. Eng. Part B J. Eng. Manuf. 236 (2021) 946–954. doi:10.1177/09544054211056420.
[14] P. Ranjan, R. Balasubramaniam, V.K. Jain, Molecular dynamics simulation of mechanical polishing on stainless steel using diamond nanoparticles, J. Manuf. Sci. Eng. Trans. ASME. 141 (2019). doi:10.1115/1.4041914.
[15] P. Ranjan, A. Sharma, T. Roy, R. Balasubramaniam, V.K. Jain, Molecular dynamics simulation of mechanical polishing, Int. J. Precis. Technol. 8 (2019) 335. doi:10.1504/ijptech.2019.10022599.
[16] P. Ranjan, R. Balasubramaniam, V.K. Jain, Mechanism of material removal during nanofinishing of aluminium in aqueous KOH: A reactive molecular dynamics simulation study, Comput. Mater. Sci. 156 (2019) 35–46. doi:10.1016/j.commatsci.2018.09.042.
[17] D.P. Ranjan, M.A. Owhal, D. Chakrabarti, D.S. Belgamwar, T. Roy, D.R. Balasubramaniam, Fundamental Insights of Mechanical Polishing on Polycrystalline Cu Through Molecular Dynamics Simulations, SSRN Electron. J. (2022). doi:10.2139/ssrn.4062796.
[18] G. Bonny, D. Terentyev, R.C. Pasianot, S. Poncé, A. Bakaev, Interatomic potential to study plasticity in stainless steels: the FeNiCr model alloy, Model. Simul. Mater. Sci. Eng. 19 (2011) 085008. doi:10.1088/0965-0393/19/8/085008.
[19] J. Tersoff, Modeling solid-state chemistry: Interatomic potentials for multicomponent systems, Phys. Rev. B. 39 (1989) 5566–5568. doi:10.1103/PhysRevB.39.5566.
[20] J. Xie, Atomistic Simulations and Experimental Studies of Transition Metal Systems Involving Carbon and Nitrogen, Royal Institute of Technology, Stockholm, Sweden, 2006.
[21] A. V. Verkhovtsev, S. Schramm, A. V. Solov'Yov, Molecular dynamics study of the stability of a carbon nanotube atop a catalytic nanoparticle, Eur. Phys. J. D. 68 (2014). doi:10.1140/epjd/e2014-50371-4.
[22] J. Stadler, R. Mikulla, H.R. Trebin, IMD: A software package for molecular dynamics studies on parallel computers, Int. J. Mod. Phys. C. 8 (1997) 1131–1140. http://apps.isiknowledge.com/full_record.do?product=WOS&search_mode=GeneralSearch&qid=51&SID=W1ki6LhmKpGP@h3A2HP&page=1&doc=8.
[23] A. Stukowski, Visualization and analysis of atomistic simulation data with OVITO–the

Open Visualization Tool, Model. Simul. Mater. Sci. Eng. 18 (2009) 015012. doi:10.1088/0965-0393/18/1/015012.
[24] A.K. Subramaniyan, C.T. Sun, Continuum interpretation of virial stress in molecular simulations, Int. J. Solids Struct. 45 (2008) 4340–4346. doi:10.1016/j.ijsolstr.2008.03.016.
[25] A. Stukowski, V. V. Bulatov, A. Arsenlis, Automated identification and indexing of dislocations in crystal interfaces, Model. Simul. Mater. Sci. Eng. (2012). doi:10.1088/0965-0393/20/8/085007.
[26] N. Taniguchi, Nano-machining or processing systems of nanometre accuracies and sub-nanometre scattering width or processing resolutions, in: Nanotechnol. Inegrated Process. Syst. Ultra-Precision Ultra-Fine Prod., First, Oxford University Press, New Delhi, 2008: pp. 15–17.
[27] P.S. Martins, S.S. Pires, E. Rodrigues da Silva, V.F. Vieira, E.C. Talibouya Ba, C.A. Rodrigues Dias, Tribological aspects of the Diamond-like carbon film applied to different surfaces of AISI M2 steel, Wear. (2022). doi:10.1016/j.wear.2022.204469.